Submitted to

International Europhysics Conference on High Energy Physics, EPS03, July 17-23, 2003, Aachen
(Abstract **093** Parallel Session **4**)

XXI International Symposium on Lepton and Photon Interactions, LP03, August 11-16, 2003, Fermilab

www-h1.desy.de/h1/www/publications/conf/conf_list.html

Measurement of Prompt Photon Production in γp Interactions

H1 Collaboration

Abstract

Results are presented on the photoproduction of isolated prompt photons, both, inclusively and associated with jets in the γp center of mass energy range $142 < W < 266$ GeV. The cross sections are given for the transverse momentum and pseudorapidity ranges of the photons $5 < E_T^\gamma < 10$ GeV, $-1 < \eta^\gamma < 0.9$ and for the associated jets in the range $E_T^{jet} > 4.5$ GeV, $-1 < \eta^{jet} < 2.3$ as a function of $E_T^\gamma, \eta^\gamma, E_T^{jet}, \eta^{jet}, x_p$ and x_γ, where x_p and x_γ correspond to the energy fractions of the incident proton and exchanged photon, respectively, participating in the hard process. The results are reasonably well described by pQCD calculations in next to leading order. The data were taken at HERA in the years 1996-2000 corresponding to an integrated luminosity of 105 pb^{-1}.

1 Introduction

High energy ep collisions at HERA proceed mainly through electron[1] scattering at small angles where a quasi real photon emitted by the incoming electron interacts with the proton. The interaction of the partons of the quasi real photon and of the proton can lead to the process of so called prompt photon emission which is sensitive to their partonic substructures. An isolated photon at large transverse energy E_T^γ can be related directly to the partonic event structure which is in contrast to jet measurements where the partonic structure is hidden behind the non perturbative hadronisation process. However, further information on the dynamics of the process can be obtained if prompt photons are measured together with jets.

Next to leading order (NLO) perturbative QCD (pQCD) calculations for inclusive production of isolated photons are available [1–4]. In such calculations the exchanged photon interacts with the partons of the proton either directly or as a resolved photon. The final state photon can be emitted in a hard partonic process or can be produced in a fragmentation process of a quark or gluon.

In this paper, the previously reported results on inclusive prompt photon production [5] are presented together with data where in addition to the photon a jet is detected. We confront the measurements with NLO calculations using the program of Fontannaz, Guillet and Heinrich [1, 2] and with the event generator PYTHIA [6] based on leading order QCD matrix elements and leading logarithmic parton showers. The results are also compared to data of the ZEUS collaboration [7].

2 Strategy of Prompt Photon Measurement

Prompt photons are identified in the H1 liquid argon (LAr) calorimeter [8]. The main experimental difficulty is the separation of prompt photons from hadronic background, in particular from signals due to π^0 mesons, as for those, at high energies, the two energetic decay photons cannot be resolved in the calorimeter. The π^0 mesons are predominantly produced in jets. Therefore an isolation requirement is applied for the γ candidates.

No track is allowed to point to the calorimetric energy cluster of the γ candidate to exclude events in which the cluster is faked by electrons. Neutral current (NC) deep inelastic scattering (DIS) background events are further reduced by requiring a significant energy loss in the electron beam direction as expected in photoproduction from the unmeasured energy of the electron scattered under small angles.

After all selection cuts, the background is still of similar size to the prompt photon signal. The signal is thus extracted exploiting a combination of discriminating shower shape functions. Distributions of the γ candidates are fitted by a sum of contributions of simulated photons, π^0 and η mesons. This procedure is applied two-dimensionally in bins of transverse energy E_T^γ and pseudorapidity η^γ. [2]

[1]The term “electron” is used for electrons and positrons.

[2]The pseudorapidity η of an object with polar angle θ is given by $\eta = -\ln\ \tan(\theta/2)$, where θ is measured with respect to the z axis given by the proton beam direction.

The data are corrected for detector effects by a detailed simulation of prompt photon production in the H1 detector based on the PYTHIA event generator [6]. The π^0 and η background estimate of PYTHIA is not used in the analysis. Only the η/π^0 fraction in the background ($\approx 5\%$ after selection) is taken from the generator.

3 Event Selection

The data have been collected with the H1 detector [9] at HERA in different data taking periods with electrons or positrons with energy $E_e = 27.6$ GeV collided with protons of energies $E_p = 820$ GeV or $E_p = 920$ GeV. The data correspond to an integrated luminosity of $105\ \mathrm{pb}^{-1}$ of which $28.8\ \mathrm{pb}^{-1}$ and $61.3\ \mathrm{pb}^{-1}$ are recorded in e^+p interactions at center of mass energies $\sqrt{s} = 301$ GeV and $\sqrt{s} = 319$ GeV respectively, and $14.9\ \mathrm{pb}^{-1}$ in e^-p interactions at $\sqrt{s} = 319$ GeV.

The main experimental requirements for the event selection are the following:

- The events are triggered by compact energy depositions in the LAr calorimeter.
- A compact electromagnetic energy cluster, consistent with a γ shower, is reconstructed in the LAr calorimeter in the range $E_T^\gamma > 5$ GeV and $-1 < \eta^\gamma < 0.9$. No track is allowed to point to this cluster within a distance of 25 cm.
- Events with electron candidates are rejected, which restricts the virtuality of the exchanged photon to $Q^2 < 1\ \mathrm{GeV}^2$.
- An event vertex is required to be within ± 35 cm in z of the nominal vertex position to remove non ep background.
- At least two tracks in the central tracker are required, which assures good vertex reconstruction and suppresses QED Compton background.
- For the inelasticity $y = 1 - E_e'/E_e$ we require $0.2 < y < 0.7$, where E_e' is the energy of the non-detected scattered electron. The inelasticity is evaluated as $y = \sum (E - p_z)/2E_e$ where the sum runs over all detected final state particles. The range of y corresponds to the γp center of mass energy range $142 < W < 266$ GeV at $E_p = 920$ GeV.
- The γ candidate is required to be isolated. The transverse energy, E_T^{cone}, in a cone around the γ candidate, given by distances below 1 unit in the $(\eta - \phi)$ plane, is required not to exceed 10% of E_T^γ , following the convention of [7].
- Associated jets are reconstructed using the inclusive k_T algorithm [10] with the conditions $E_T^{jet} > 4.5$ GeV and $-1 < \eta^{jet} < 2.3$ for the jet energy and pseudorapidity respectively.

4 Signal Extraction

A large fraction of the selected γ candidates have showers initiated by π^0 mesons. The fraction of prompt photons in the data is extracted by a shower shape analysis where the mean transverse shower radius given by $R = \sum_i r_i \varepsilon_i / \sum_i \varepsilon_i$ and the "shower hot core fraction" (HCF) are used to discriminate against background. Here r_i is the transverse distance of cell i with energy density ε_i measured with respect to the axis from the event vertex to the center of gravity of the γ candidate cluster. HCF is the energy fraction of the cluster which is contained in 4 or 8 contiguous cells including the cell of highest energy depending on calorimeter granularity. Discriminating functions based on the distributions of R and HCF are calculated for the data and for simulated samples of photons, π^0 mesons and η mesons. The contribution of the different particle types is then determined by fits to the data distributions independently in 6×6 bins in η^γ and E_T^γ. The η/π^0 fraction ($\approx 5\%$ after selection) is taken from PYTHIA.

The measured distributions of R and HCF for the full η^γ, E_T^γ range are shown in Fig. 1 together with the simulated distributions of photons and background from π^0 and η mesons. For the latter the normalisations are taken from the discriminating fits described above. The data distribution is well described by the extracted signal and background components. The discrimination power decreases at high E_T^γ where the R and HCF distributions of π^0 mesons and photons get more similar. Therefore events with $E_T^\gamma > 10$ GeV are not included in the results presented below.

5 Systematic Uncertainties

For the prompt photon cross sections various systematic uncertainties were considered and the total systematic errors are obtained by adding the different systematic errors in quadrature.

- The most important systematic errors are due to imperfections in the simulation of the shower shapes. Uncertainties in the simulated distributions of R and HCF have been estimated by comparing simulations of electrons with electron candidates in NC DIS events. Differences in these distributions have been quantified resulting in errors on the cross sections ranging from $\pm 10\%$ to $\pm 20\%$.
- The uncertainties on the calorimeter electromagnetic and hadronic energy scales contribute errors of about 5% to the inclusive cross sections. For the case of associated jets the hadronic energy uncertainty contributes about 10%.
- Background due to DIS electrons resulting from the tracker inefficiency (below 0.4% for the track selection used) leads to a subtraction of 3.0% with an uncertainty of $\pm 0.3\%$ in the lowest η bin and at high E_T^γ , and is negligible otherwise.
- An overall normalisation uncertainty of $\pm 1.5\%$ on the luminosity measurement is not included in the results.

- To take account of model dependencies in the detector corrections, which are determined by simulation of the measurement using PYTHIA, the shape of the E_T^γ dependence in PYTHIA is varied leading to uncertainties below 3%. Also the sensitivity of the detector corrections to the underlying event activity in PYTHIA is studied by changing the relative weight of the PYTHIA events in proportion to the transverse energy E_T^{cone} in the isolation cone around the photon. Allowing a change for the relative event yield at the cut energy $E_T^{cone} = 0.1 \cdot E_T^\gamma$ by factors 0.5 and 2 leads to variations of the final results below 3% which are included in the systematic errors. It was verified that PYTHIA gives a good description of the dependence of the measured cross sections on the chosen cut on the isolation cone.

6 Results

The results are presented as ep cross sections [3] for

$$\sqrt{s} = 319 \text{ GeV}, \;\; 0.2 < \mathrm{y} < 0.7, \;\; \mathrm{Q}^2 < 1 \text{ GeV}^2, \; 5 < \mathrm{E_T^\gamma} < 10 \text{ GeV}, \; -1 < \eta^\gamma < 0.9$$

$$\text{including the photon isolation condition } E_T^{cone} < 0.1 \;\cdot E_T^\gamma.$$

The errors in the figures contain the statistical errors as obtained from the shower discriminating fits and the systematic errors added in quadrature.

Inclusive differential cross sections $\mathrm{d}\sigma/\mathrm{d}E_T^\gamma$ and $\mathrm{d}\sigma/\mathrm{d}\eta^\gamma$ are shown in Fig. 2 and compared to the NLO pQCD calculation of Fontannaz et al. [1] and the PYTHIA event generator [6]. In the NLO calculation E_T^γ is used for the renormalisation and the factorisation scales. The photon and proton parton densities AFG [11] and MRST2 [12] are used respectively. In PYTHIA the leading order QCD matrix elements are regulated by a minimum cut-off in transverse momentum which is set to 3 GeV. The parton densities GRV(LO) [13, 14] are used for the photon and proton. The program simulates multiple parton interactions (MI) and initial and final state QED and QCD radiation [4].

The NLO calculation describes the data quite well in the presented E_T^γ and η^γ ranges with a tendency to overshoot the data at large η^γ. The PYTHIA simulation describes the data well in shape, but is low by about 30% in normalisation. For comparison we show in Fig. 3 also the PYTHIA prediction without multiple interactions. It is interesting to note that in this case the predictions at $0 < \eta^\gamma < 0.9$ are about 25% higher, showing that the cross section is reduced by the soft underlying event activity, as expected [1] due to the isolation condition. Fig. 3 shows the full PYTHIA prediction with and without MI, as well as the separate contributions of resolved interactions of the exchanged photon and of photon radiation from a final state quark in di-jet events.

[3] The cross sections obtained at $\sqrt{s} = 301$ GeV are transformed to $\sqrt{s} = 319$ GeV by corrections of about $+4\%$ taken from PYTHIA.

[4] PYTHIA 6.15/70 was used with default parameters except $< k_T^2 >= 1$ GeV^2 for the intrinsic k_T of initial state partons in the proton.

The data are compared[5] to the results of the ZEUS collaboration in Fig. 4 at $\sqrt{s} = 301$ GeV in the range $-0.7 < \eta^\gamma < 0.9$ and $0.2 < y < 0.9$. The data are consistent, but the H1 data are somewhat lower at small η^γ, where the ZEUS results appear to exceed the NLO calculation.

Cross sections for a prompt photon together with a jet are presented in Fig. 5 as a function of the variables $E_T^\gamma, \eta^\gamma, E_T^{jet}, \eta^{jet}, x_p$ and x_γ, where $x^p = (E_T^{jet} e^{\eta^{jet}} + E_T^\gamma e^{\eta^\gamma})/2E_p$ and $x_\gamma = (E_T^{jet} e^{-\eta^{jet}} + E_T^\gamma e^{-\eta^\gamma})/2yE_e$ correspond to the energy fractions of the incident proton and exchanged photon, respectively, participating in the hard process. The NLO corrections are substantial and lead to a good description of the data. Taking into account the multiple interaction effects, as expected on the basis of PYTHIA, improves the data description in particular at $\eta^\gamma > 0$ and $x_\gamma < 0.5$. No corrections have been made to the NLO prediction for hadronisation effects.

A measurement with jet energy $E_{T,min}^{jet} = 5$ GeV is shown differentially in E_T^γ in Fig. 6. As also observed in dijet analyses, the data can not be directly described by NLO calculations in the region of symmetric cuts $E_{T,min}^{jet} = E_{T,min}^\gamma$. Infrared instabilities lead to an unphysical drop of the calculated NLO cross section near the cut value, as discussed in [2].

7 Conclusions

Photoproduction of prompt photons, both, inclusively and associated with jets, has been studied. The data are quite well described in the kinematic range covered by a NLO pQCD calculation, but the prediction is above the data in the forward region ($\eta^\gamma > 0.6$) which may be related to underlying event activity not contained in the NLO calculation. The cross sections produced with the PYTHIA event generator describe the data distribution well in shape with a normalisation that is about 30% low. The presented inclusive prompt photon cross sections $\mathrm{d}\sigma/\mathrm{d}E_T^\gamma$ and $\mathrm{d}\sigma/\mathrm{d}\eta^\gamma$ are in broad agreement with results from the ZEUS collaboration, but tend to be lower at negative η^γ .

Acknowledgements

We are grateful to Gudrun Heinrich for discussions and for providing some results of the NLO QCD calculations.

References

[1] M. Fontannaz, J. P. Guillet and G. Heinrich, Eur. Phys. J. C **21** (2001) 303 [arXiv:hep-ph/0105121].

[2] M. Fontannaz, J. P. Guillet and G. Heinrich, Eur. Phys. J. C **22** (2001) 303 [arXiv:hep-ph/0107262].

[5] The H1 data are corrected for the extension of the upper limit in y from 0.7 to 0.9 using PYTHIA.

[3] M. Krawczyk and A. Zembrzuski, Phys. Rev. D **64** (2001) 114017 [arXiv:hep-ph/0105166].

[4] L. E. Gordon and W. Vogelsang, Phys. Rev. D **52**, 58 (1995).

[5] H1 Collab., contributed paper ICHEP2002 (Amsterdam), Abstract 1007.

[6] T. Sjöstrand, P. Edén, C. Friberg, L. Lönnblad, G. Miu, S. Mrenna and E. Norrbin, Comput. Phys. Commun. **135** (2001) 238 [arXiv:hep-ph/0010017].

[7] J. Breitweg *et al.* [ZEUS Collaboration], Phys. Lett. B **472** (2000) 175 [arXiv:hep-ex/9910045].

[8] B. Andrieu *et al.* [H1 Calorimeter Group Collaboration], Nucl. Instrum. Meth. A **336** (1993) 460.

[9] I. Abt *et al.* [H1 Collaboration], Nucl. Instrum. Meth. A **386** (1997) 310; ibid. A **386** (1997) 348.

[10] S. D. Ellis and D. E. Soper, Phys. Rev. D **48** (1993) 3160 [arXiv:hep-ph/9305266].

[11] P. Aurenche, J. P. Guillet and M. Fontannaz, Z. Phys. C **64** (1994) 621 [arXiv:hep-ph/9406382].

[12] A. D. Martin, R. G. Roberts, W. J. Stirling and R. S. Thorne, Eur. Phys. J. C **14** (2000) 133 [arXiv:hep-ph/9907231].

[13] M. Glück, E. Reya and A. Vogt, Phys. Rev. D **46**, 1973 (1992).

[14] M. Glück, E. Reya and A. Vogt, Z. Phys. C **67** (1995) 433.

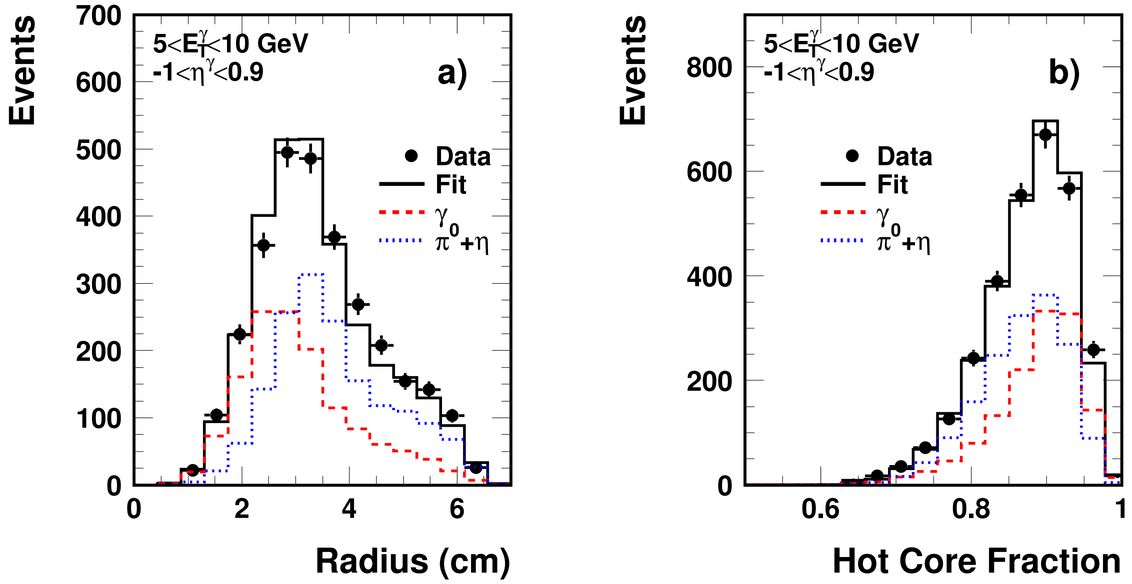

Figure 1: Distributions of the mean transverse shower radius R (a) and and the hot core fraction HCF (b) for the selected photon candidates (data points) for the full range $-1 < \eta < 0.9,\ 5 < E_T^\gamma < 10$ GeV. Also shown are the results of the fit (solid lines) by the extracted contributions of photons (dashed lines) and background ($\pi^0 + \eta$, dotted lines) (see text).

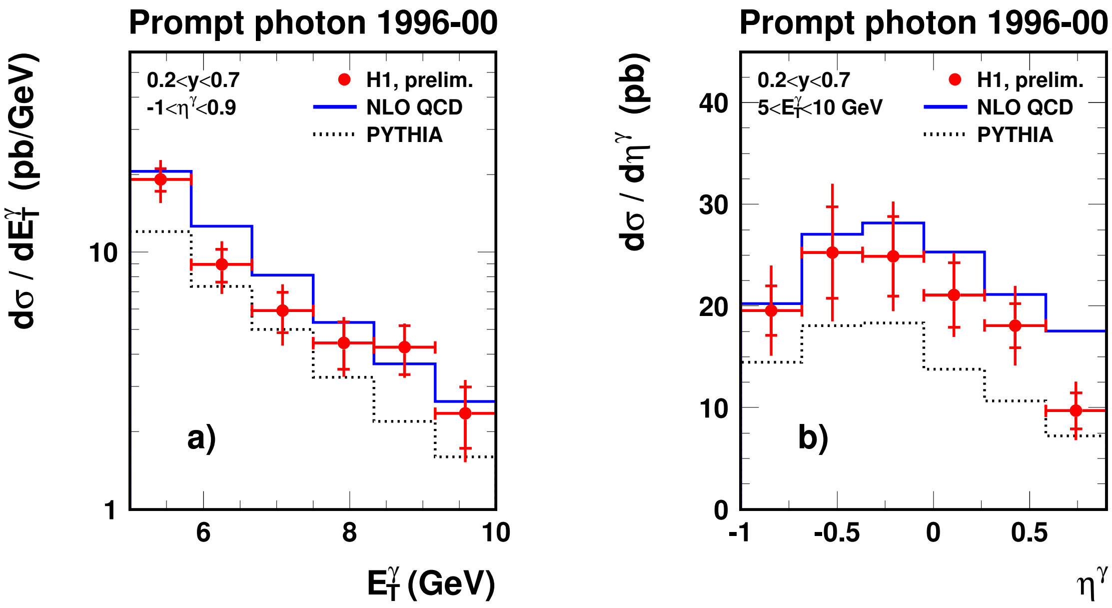

Figure 2: Inclusive prompt photon differential cross sections $\mathrm{d}\sigma/\mathrm{d}E_T^\gamma$ for $-1 < \eta^\gamma < 0.9$ (a) and $\mathrm{d}\sigma/\mathrm{d}\eta^\gamma$ for $5 < E_T^\gamma < 10$ GeV (b) at $\sqrt{s} = 319$ GeV and $0.2 < y < 0.7$ compared to the prediction of a NLO pQCD calculation [1] and the PYTHIA generator [6].

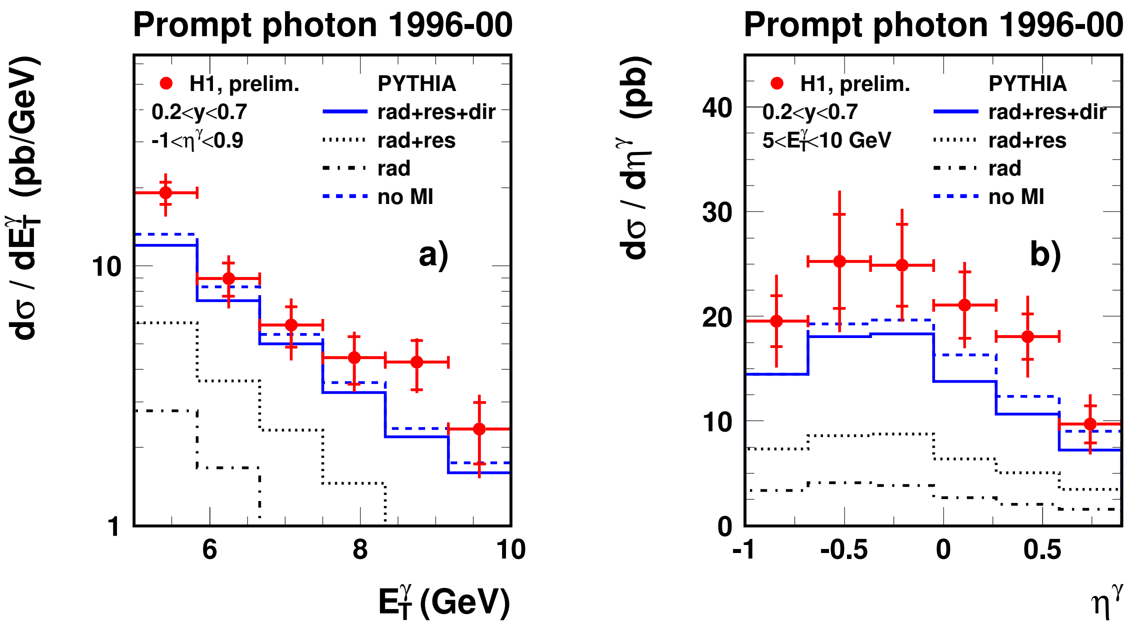

Figure 3: Inclusive prompt photon differential cross sections $\mathrm{d}\sigma/\mathrm{d}E_T^\gamma$ for $-1 < \eta^\gamma < 0.9$ (a) and $\mathrm{d}\sigma/\mathrm{d}\eta^\gamma$ for $5 < E_T^\gamma < 10$ GeV (b) at $\sqrt{s} = 319$ GeV and $0.2 < y < 0.7$ compared to the PYTHIA prediction including multiple interactions (full line), with the contributions from di-jet events where a final state quark radiates a photon (dashed-dotted) and this component summed with resolved photon events (dotted line). Also shown is the the full PYTHIA prediction without multiple interactions (dashed line).

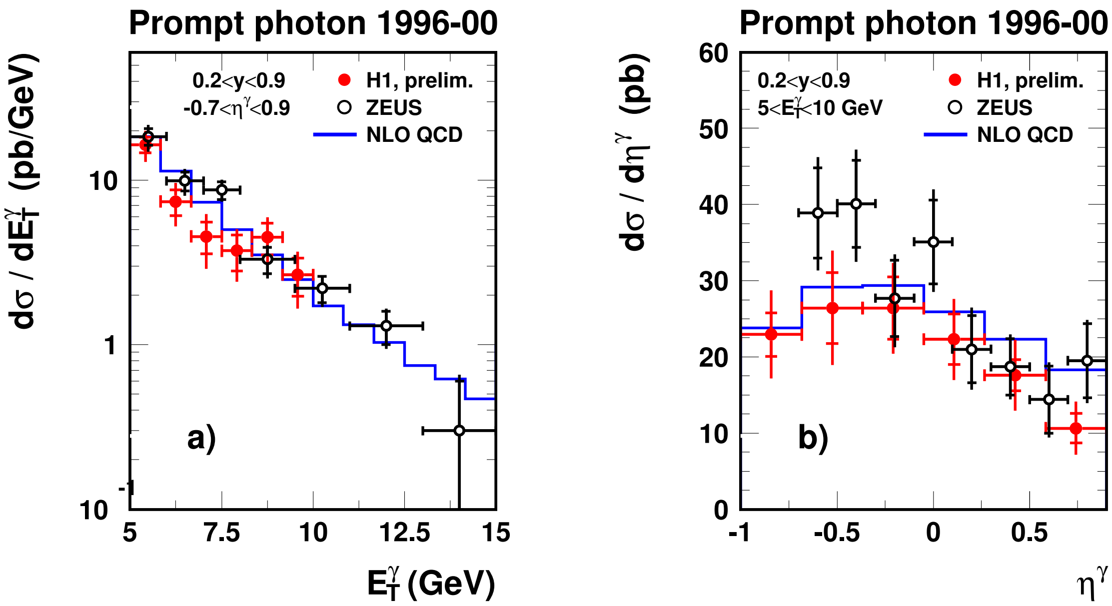

Figure 4: Inclusive prompt photon differential cross sections $\mathrm{d}\sigma/\mathrm{d}E_T^\gamma$ for $-0.7 < \eta^\gamma < 0.9$ (a) and $\mathrm{d}\sigma/\mathrm{d}\eta^\gamma$ for $5 < E_T^\gamma < 10$ GeV (b) corrected to $\sqrt{s} = 301$ GeV and $0.2 < y < 0.9$, compared to results of the ZEUS collaboration [7]. Also shown is the prediction of a NLO pQCD calculation [1].

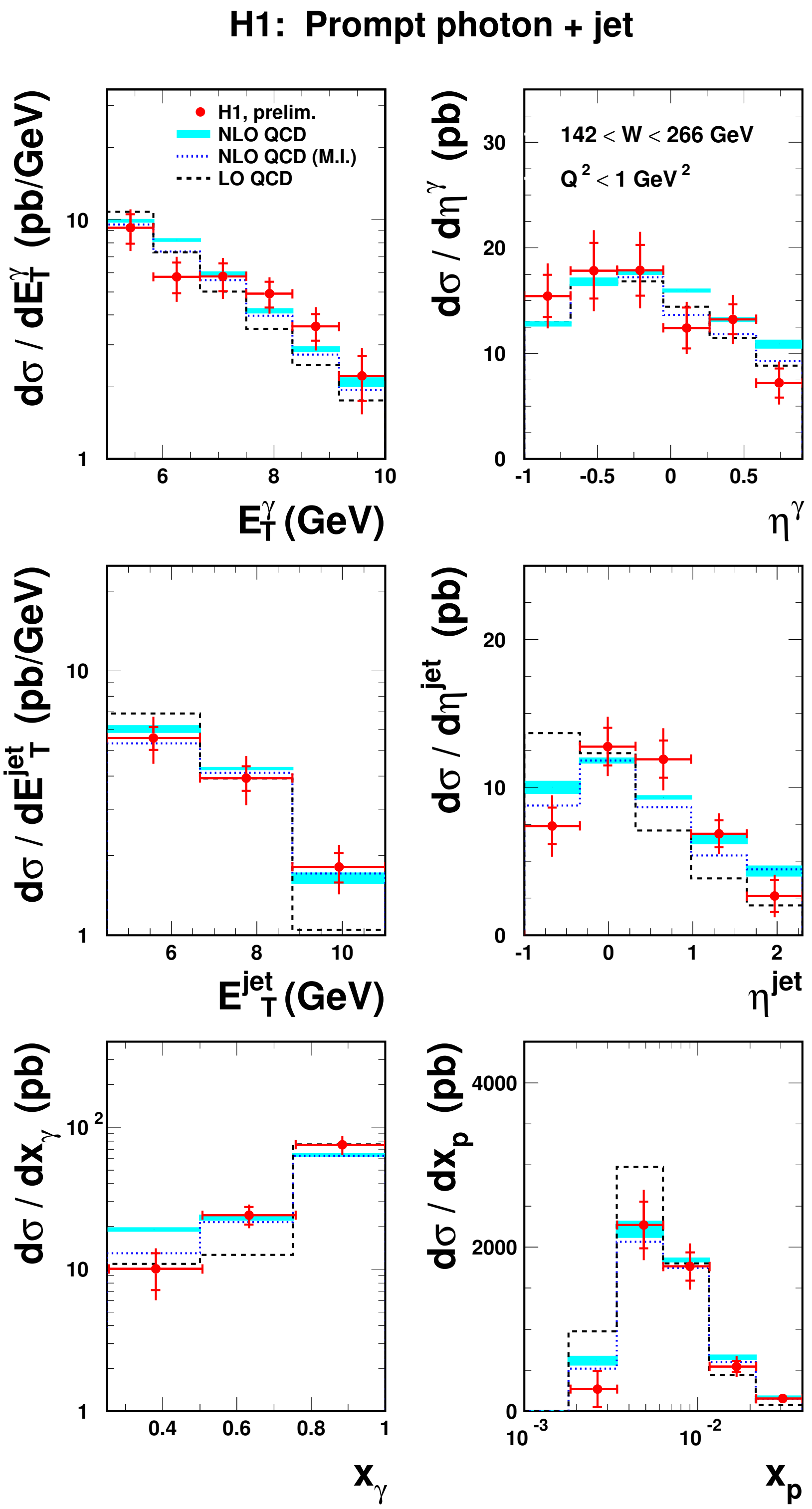

Figure 5: Prompt photon differential cross sections with an additional jet requirement ($E_T^{jet} > 4.5$ GeV) as a function of E_T^γ, η^γ, E_T^{jet}, η^{jet}, x_γ, and x_p. The data are compared with pQCD in LO (dashed line) and NLO [1, 2]. The error bands show the effect of a variation of the renormalisation and factorisation scales in the NLO calculation from $0.5 \cdot E_T^\gamma$ to $2 \cdot E_T^\gamma$. Also shown is the NLO result corrected by PYTHIA for multiple interaction effects (NLO QCD (M.I.), dotted line).

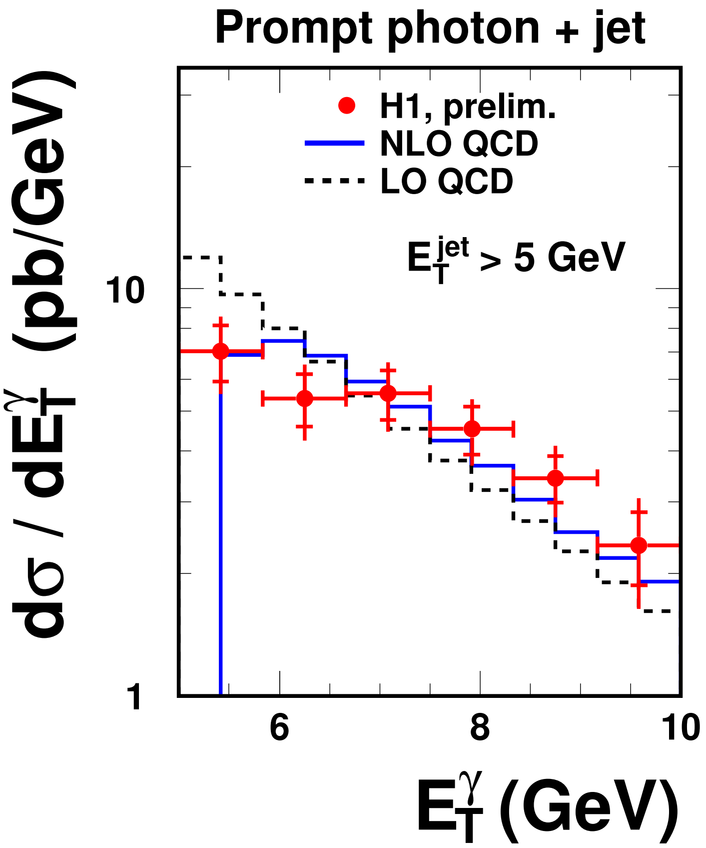

Figure 6: Prompt photon differential cross sections with a jet requirement as function of E_T^γ with $E_{T,min}^{jet} = E_{T,min}^{\gamma} = 5$ GeV. The data are compared with pQCD LO (dashed line) and NLO (solid line) [1, 2].